

Climate-induced severe water scarcity events as harbinger of global grain price

Miroslav Trnka (✉ mirek_trnka@yahoo.com)

Global Change Research Institute, Czech Academy of Sciences & Mendel University in Brno
<https://orcid.org/0000-0003-4727-8379>

Jan Meitner

Global Change Research Institute, Czech Academy of Sciences & Mendel University in Brno

Jan Balek

Global Change Research Institute, Czech Academy of Sciences & Mendel University in Brno

Song Feng

Juliana Arbelaez-Gaviria

Global Change Research Institute, Czech Academy of Sciences & Mendel University in Brno
<https://orcid.org/0000-0001-8440-1933>

Milan Fischer

Global Change Research Institute, Czech Academy of Sciences & Mendel University in Brno

Esther Boere

International Institute of Applied Systems Analysis

Petr Havlík

International Institute for Applied Systems Analysis <https://orcid.org/0000-0001-5551-5085>

Kurt Kersebaum

Leibniz Centre for Agricultural Landscape Research <https://orcid.org/0000-0002-3679-8427>

Claas Nendel

Leibniz Centre for Agricultural Landscape Research (ZALF) <https://orcid.org/0000-0001-7608-9097>

Margarita Ruiz-Ramos

Universidad Politécnica de Madrid/ ETSI Agrónomos <https://orcid.org/0000-0003-0212-3381>

Daniela Semerádová

Global Change Research Institute, Czech Academy of Sciences & Mendel University in Brno

Mikhail Semenov

Rothamsted Research <https://orcid.org/0000-0002-1561-7113>

Markéta Poděbradská

Global Change Research Institute, Czech Academy of Sciences & Mendel University in Brno

Jan Esper

Johannes Gutenberg University <https://orcid.org/0000-0003-3919-014X>

Ulf Buentgen

University of Cambridge <https://orcid.org/0000-0002-3821-0818>

Max Torbenson

Johannes Gutenberg University Mainz <https://orcid.org/0000-0003-2720-2238>

Jáchym Brzezina

Global Change Research Institute, Czech Academy of Sciences

Zdeněk Žalud

Global Change Research Institute, Czech Academy of Sciences & Mendel University in Brno

Gabriel Katul

Duke University

Jorgen Olesen

Aarhus University <https://orcid.org/0000-0002-6639-1273>

Article**Keywords:**

Posted Date: September 19th, 2023

DOI: <https://doi.org/10.21203/rs.3.rs-3293805/v1>

License:   This work is licensed under a Creative Commons Attribution 4.0 International License.

[Read Full License](#)

Abstract

The severe water scarcity (SWS) concept allows for consistent analysis of the supply and demand for water sourced grain production worldwide. Thus, the primary advantage of using SWS is its ability to simultaneously accommodate the spatial extent and temporal persistence of droughts using climatic data. The SWS concept was extended here to drivers of global grain prices using past SWS events and prices of three dominant grain crops: wheat, rice and maize. A significant relation between the SWS-affected area and the prices of wheat was confirmed. The past price–SWS association was then used to project future wheat prices considering likely climate change scenarios until 2050 and expected SWS extent. The projected wheat prices increase with increasing SWS area that is in turn a function of greenhouse gas emissions. The need to act to reduce greenhouse gas emissions is again reinforced assuming the SWS-price relation for wheat is unaltered.

Introduction

Wheat, maize and rice account for 42% of the global societal dietary energy supply and 37% of the global protein supply (Fig. 1a)¹. Wheat is the main source of protein for humans (19%), and rice and wheat combined remain the dominant sources of calories (37%, respectively)¹. Thus, the prominence of cereals in the global food system is not in dispute. The sheer scale of cereal production and land use underscores this point. Some 35% of cropland where wheat is the most common crop accounts for 218 million hectares (Fig. 1a). Wheat and rice are also associated with the highest combined blue water (i.e., fresh surface and groundwater) use and together with maize account for 51% of the global blue water footprint². Any change in the water availability (or lack thereof) will impact the production, availability, and price of these crops.

By mid-century, the Food and Agriculture Organization (FAO) projects an increase of 40% in the food and agricultural product demand when compared to 2020 levels. Wheat will be the most consumed cereal as food (0.6 Gt), and maize will be the most consumed cereal as feed (0.97 Gt)³. The necessary increases in the agricultural output driven by this demand will likely be achieved by yield increases rather than cultivated land expansion. This change will primarily occur in emerging economies presumably by improving various technologies and cultivation practices, including mobilizing production resources such as irrigation water and fertilizer⁴. The challenge of maintaining a balance between the cereal demand and supply under a changing climate is evident^{5–7} with a particular concern raised regarding available water resources^{8,9} (quantity and quality).

Approximately 14% of the global cereal production is traded internationally, and 90% of these exports are generated by ten producing countries. Global prices are assumed closely linked to the current environmental conditions in these countries⁹. While the production of wheat, maize, and rice steadily grew over the past 60 years, the prices of these cereals showed a marginal overall increase between 1960 and 2000 followed by significant increases over the past 22 years. Among the three crops, wheat is a

particularly volatile commodity¹⁰ exhibiting punctuated growth. During the grain price crises of 2007/08 and 2010/11, wheat prices increased by 137% and 72%, respectively, relative to the preceding years. In comparison, rice prices changed by only 85% and 4%, respectively, and maize prices by 35% and 72%, respectively^{*,11}. Of far greater concern is the number of undernourished individuals. This number increased from 848 million in 2005–2007 to 1023 million by 2009^{12,13}, which far exceeds the global population increase during the same period

The growing demand for cereals and their high price volatility are only part of any future challenges to food security. Crop models predict 1.5%, 15.5%, and 6.7% decreases in global rice, maize, and wheat productivity levels, respectively, per 1°C of warming without adaptation¹⁴. These model projections of cereal productivity consider key factors such as hydroclimatic variability such as air temperature and vapor pressure deficit, soil water conditions, irrigation, crop cultivar and management practices, and even the effects of increasing atmospheric CO₂ concentration levels on photosynthesis and water-use efficiency. However, these projections must be viewed as incomplete because they fail to account for occurrences of large-scale adverse climate extremes^{8,15} that can be persistent over extended durations coinciding with particular crop-growth stage. Although global warming is expected to increase the frequency of extreme events, most projections of climate change impacts on agricultural commodity prices consider only long-term yield trends based on multiyear means^{16,17}. Thus, these projections remain silent on the role of intensive, longer-lasting, larger-scale or co-occurring extreme events¹⁴. The spatiotemporal relations of such events and their compound impact on grain prices continue to be a formidable scientific challenge and a knowledge barrier. As a logical starting point to address these challenges, the work here seeks to bridge the influence of climate change along with its resulting coherent spatio-temporal extremes directly on cereal prices. This aim was achieved by first determining whether soil water content anomalies expressed as severe water scarcity (SWS) events notably affected historic cereal prices and then proceeding to estimate changes in 2050 price levels driven by expected water scarcity increases as derived from climate projections. .

Results

Sensitivity of global rice, maize and wheat prices to SWS

To estimate the influence of SWS events (defined as an unusually low water availability in Table S1) on grain prices, SWS was analyzed at three spatial scales by averaging over (i) the total arable land; (ii) growing area for each crop; and (iii) crop-growing areas of the top ten global exporters (Fig. S1). The analysis showed that for rice, none of these approaches yielded significant results (Fig. 1b). The maize price models explained up to 40% of the global price variability ($p < 0.01$), with the SWS extent in maize-growing regions being the most efficient predictor. These predictions were no less effective when only SWS affected maize growing area of the top ten exporters was used (Fig. 1b). Regarding wheat, the relation between the SWS-affected area and fluctuations in global prices was closer than that in the case of maize (Fig. 1b and Table S2). The highest explained variance in the wheat grain price (65%) and the

smallest root mean square error (RMSE) were achieved when considering the SWS area in the top ten exporting countries.

The different sensitivities of rice, maize and wheat prices to SWS occurrence were at least partly explained in Fig. 1c. Rice is predominantly grown in environments (Fig. 1c) where rainfall exceeds the potential evapotranspiration (PET) during the critical part of the growing season defined as four months prior to harvest. This is in direct contrast to wheat, which is grown in cooler environments under mostly water-limited conditions. These areas are characterized by climates with higher PET levels than rainfall. Maize is grown in transition zones between these two endmember situations. The SWS influence on rice is also partially offset by irrigation, which covers 33% of the total harvested area of this grain and only 15% of that of wheat¹⁸. The overall results confirmed the SWS rationale when the SWS–price responses of all three crops were compared. As wheat is grown in areas with the least favorable water balance (Fig. 1c) and is the least affected by irrigation, further analyses of the SWS effect on grain prices focused on wheat.

Estimating the wheat price response to SWS variation

Five SWS–wheat price models were used to estimate the effect of the variation in the SWS-affected area (Figs. 1b and S3) on wheat grain prices (Fig. 2a). These SWS–wheat price models individually explained between 52% and 65% of the price variability (Fig. S4 and Table S2). However, all models underestimate the impact of high SWS exposure on price variability. The five-model ensemble explained 72% of the interannual wheat price variability from 2000 to 2021 with a relative RMSE of 27.6% for the wheat price (Fig. 2a), expressed in terms of the wheat price index (WPI). The relation between SWS and global wheat price remained statistically significant ($p < 0.001$) even if the years of peak prices, namely, 2007/2008, 2010/2011, 2018/2019, and 2019/2020, were excluded. The results indicated not only that SWS variations affect the global wheat grain price but also that wheat grain prices are closely related to SWS events in the top-ten wheat exporting countries (Fig. S3).

Observed and expected shifts in the SWS extent and impact on the wheat grain price

Between 1911 and 2020, $5.0\% \pm 4.2\%$ of the global wheat-growing area was affected by SWS on average, with the maximum extent exceeding 15% in 2000, 2010, 2012 and 2020 (Fig. S2). The average SWS-affected area exhibited a significant positive trend ($p < 0.001$) between 1911 and 2000, with a 0.5% increase of the affected climate grid cells per decade. Between 2011 and 2021, the rate of SWS area increase was even higher at some 2.2%.

Translating those changes in SWS to price changes used two indicators: the reported whole-sale price index (WPI) and a closely related quantity that measures prices received by farmers for crop sale - the farm price index (FPI). The reported WPI from 2001–2020 and FPI from 1951–2021 occurred within the 5–95% confidence interval of price estimates based on observed Climate Research Unit (CRU) data and the historical runs of global circulation models (GCMs). The FPI, WPI and CRU-based price estimates also

followed a similar pattern over the entire period (Fig. 2d). On average, the prices generated from the GCM control run were ~ 13% lower than those estimated by the price models from observed climate data and observed prices (Fig. 3a). From 1951–2000 (i.e., the period for which the SWS–price models were not calibrated), the final price model ensemble captured the changes in the mean FPI (1951–2021) at ten-year intervals (Fig. 3a, Fig. S4). On average, the prices estimated from the observed CRU gridded climate data were higher than the reported prices prior to 1990 (Fig. 3a) and the mean of the GCM-based estimates. This finding could be explained by the Coupled Model Intercomparison Project Phase 6 (CMIP6)-GCM control run results yielding a lower percentage of the SWS-affected area than that obtained based on the CRU data. Therefore, the mean prices estimated based on the GCM findings were lower than those based on the CRU estimates. However, both the FPI and WPI values occurred within the 95% confidence intervals (Fig. 2d and 3a) of the CRU-based and the CMIP6-GCM control run-based wheat price estimates.

A summary of the expected changes in wheat prices based on the CMIP6-based SWS projections is shown in Figs. 3, S5 and S6. Wheat prices are likely to increase from a mean value of $190 \pm 53\%$ (WPI; SSP1-2.6: $166 \pm 23\%$; SSP5-8.5: $165 \pm 24\%$) based on the period 2001–2020 (Fig. 3a) to $274 \pm 19\%$ (SSP1-2.6) and $309 \pm 37\%$ (SSP5-8.5) from 2031–2050 (Fig. 3b). There were no significant ($p = 0.01$) differences among the price estimates obtained by the individual shared socioeconomic pathways (SSPs) from 2011–2040, but the divergence among the SSPs sharply increased in the late 21st century (Figs. 3c, S4 and S5). The likelihood of widespread SWS events increased in some GCMs, and the upper price estimates accordingly shifted. The modeled prices exhibited slower growth up to $+1^\circ\text{C}$ of warming, with a higher rate of increase between 1 and 2°C , followed by a slightly lower rate of price growth under more intense warming (Fig. 3c). The increase in global mean temperatures by 2°C was estimated to increase grain prices by 250% over present levels (Fig. S6). However, the projected grain prices considering temperatures above 2°C over the baseline were associated with additional modeling uncertainty, as they occurred outside the range for which the SWS-WPI models were developed and tested.

Discussion

Despite its importance, the impact of changes in the climate variability on agricultural production and food security remains limited¹⁹. Traditionally, the literature on agricultural production, consumption and market impacts has concentrated on the analysis of global mean temperature changes due to climate change by implementing 30-year moving averages of crop model outputs in partial and general equilibrium economic models^{16,20}. Fig. S7 features the effect of climate change on agricultural prices obtained by such conventional economic analysis. The Global Economic Model Intercomparison Activity of the Agricultural Model Intercomparison and Improvement Project (AgMIP) produced a range of price projections by mid-century based on numerous combinations of climatic and socioeconomic factors. The ensemble of participating models (9 models: 5 computable general equilibrium [CGE] models and 4 partial equilibrium [PE] models) projected a 3–32% wheat price increase by 2050 under SSP2 and

RCP8.5, with no significant difference between the CGE and PE models relative to the baseline scenario¹⁶. The most recent study¹⁶ projected an increase in cereal prices of 1–29% across different SSPs and 3°C warming using an ensemble of eight economic models (5 PE models, 2 CGE models and 1 integrated assessment model). These studies have given little or no attention to the analysis of extremes in relevant regions either from the viewpoint of major exporting or importing regions. This has led to a gap between the increased understanding of the influence of long-term climate change on agricultural production and the economy as a whole and a lack of knowledge regarding the immediate impacts of SWS events²¹. Through a review of the effect of cereal price increases on food consumption in 162 countries, it was found that a 1% increase in cereal prices (a deviation from its long-term trend) could lower food consumption by approximately 0.61%²². Thus, according to the projections here, food consumption could decrease by 27–38% by 2050 due to droughts. In general, households spending over 50% of their income on food are at medium risk of food insecurity due to wheat price increases²³. In low-income countries, households typically spend close to 60% of their income on food (e.g., 56.4% in Nigeria), with more than a third going toward staples such as vegetables and cereals¹². Low-income households cannot switch to less expensive foods and will be forced to spend more on basic staples, lower the quality of their diets, or even limit the amount of the most inexpensive foods consumed while also reducing nonfood expenditures²⁴. The negative impacts are even worse among poor urban households who are typically net buyers of food, while households that are net sellers of agricultural and food products would raise their income¹² unless the yields were reduced by SWS events. Considering the ongoing trend of urbanization, with 68% of the global population projected to live in cities by 2050²⁵, the pool of households that will be negatively affected by increased wheat prices will also continue to increase^{26,27}.

The projected increased food price impacts of droughts and SWS events thus require urgent action in terms of adaptation measures on the one hand and disaster-relief systems on the other hand. On the adaptation side, adjusting sowing dates²⁸, changing crops and/or growing regions²⁹, upgrading and expanding storage facilities^{30,31}, and facilitating intra- and international trade activities appear to be potential strategies. Trade was demonstrated to help reduce the number of people at risk of hunger resulting from slow-onset climate change³², although increased specialization could lead to a concentration in production locations, yielding more volatile world markets (e.g., price spikes due to SWS events).

Clearly, the drought³³ or SWS extent⁹ is a significant but not unique factor affecting crop product prices. Pests and diseases, such as fungal diseases³⁴ or locust outbreaks³⁵, and economic factors, such as demand shocks, volatile oil prices and exchange rates³⁶, political and military conflicts or policy responses³⁷, play a role and may coincide with drought events. The Ukraine–Russia conflict illustrates the response of the market and its instability as both countries are major exporters of wheat and other cereals and non-cereal crops such as oilseed that is integral to many cereal based crop rotations.. The war in Ukraine has significantly impacted the price of food products³⁸, leading to increasing exports from other countries to partially compensate for the lacking supply³⁹. In comparison to March 2021, the prices

of wheat and maize rose by 58% and 38%, respectively,¹¹ in 2022. This price increase exerts the same order of magnitude of influence as changes that could partially be attributed to SWS events over the past two decades (Fig. 2c, d). Obviously, the intensity and duration of military conflicts are inherently difficult to predict. In contrast, the increased occurrence of SWS events under future climate conditions is less uncertain (Figs. 3 and S2).

Study assumptions

A series of assumptions that facilitated the analyses were necessary to bridge SWS to indices reflecting crop price variations. The assumptions were invoked to ensure that the SWS extent is primarily a function of changing climate conditions. It was assumed that the current wheat-growing areas, their relative weights and the top ten exporting countries will remain unchanged throughout the entire 21st century. Thus, the potential benefit of shifting wheat production to other agricultural land with a lower SWS probability could lower the model reliability. However, there are two findings that suggest the conclusions drawn here are less sensitive to this simplification. First, two out of the five models in the final model ensemble are based on the SWS occurrence across the entire arable land area, and thus, a change in the wheat growing area would generate no effect. Second, the data showed that there is little to be gained globally in terms of decreasing SWS exposure by shifting wheat-producing areas both within and outside the present wheat-growing areas, as SWS exposure increases at a similar pace across all regions.

Numerous studies have argued that some or all of the negative global warming impacts on wheat yields might be ameliorated by increasing atmospheric CO₂ concentrations combined with adaptation strategies^{40,41}. Although water use is reduced under elevated CO₂ levels⁴² and may alleviate moderate dry spells, recent studies have also found that drought stress, when combined with severe heat, cannot be compensated for by elevated CO₂ concentrations^{43,44}. These findings are not surprising. While the water use efficiency is proportional to the atmospheric CO₂ concentration, it is inversely proportional to the vapor pressure deficit, which is projected to exponentially increase with increasing air temperature. Additionally, some models⁴⁵ compared future drying in model simulations with and without considering plant physiology in response to increasing CO₂ levels. They found that the plant physiological response to increasing CO₂ concentrations was secondary, suggesting that the impact of CO₂ fertilization on the future drought severity is limited. It was therefore assumed that the effects of SWS estimated here cannot be alleviated by enhanced CO₂ levels and that SWS represents a reliable indicator of drought irrespective of CO₂ levels.

It is also likely that increased temperatures will accelerate crop development, leading to earlier maturity, which might lead to avoiding SWS events for wheat crops by shifting and/or shortening the crop-growing season. Therefore, the effect of shifting the harvest earlier in the year was evaluated. While a significant reduction in the extent of the SWS-affected area was found, the advancement in the harvest date was insufficient in terms of reducing the SWS-affected areas to the levels from 1951–1990, as already shown

elsewhere⁹. In addition, significant shifts in the cropping calendar would affect not only wheat crops but also entire crop rotations, and there is high uncertainty in how these shifts will eventually occur in many regions worldwide⁴⁰.

The empirical makeup of the model assumes that the exporting countries in the future will not change relative to the present (Fig. 1 and S1). In the case of wheat, North America, the European Union, and Russia represent approximately 70% of global exports (Fig. S8). Notably, cereal yields are characterized by large differences between high- and low-income countries³. In 2018, the average grain yield in high-income countries was fourfold that in low-income countries. Closing the yield gaps across wheat-growing areas could be an efficient way to increase the resilience toward SWS-driven price increases. Major shifts in the patterns of exporting countries will, however, require substantial infrastructure investment (storage, port facilities, etc.) to allow these countries meaningful access to global markets. Interestingly, the increase in the SWS-affected area under future scenarios is so widespread that increasing the resilience of wheat to SWS by rearranging production among the top producing areas would generate only limited benefits or would have to occur at the expense of other crops, i.e., maize and rice. In this study, a constant final use of these crops was also intrinsically assumed. Dietary change toward more animal products in low-income countries or more sustainable diets in the most developed countries was not considered.

It was further assumed that the extent and influence of irrigation will not significantly change. Importantly, the global extent of irrigated croplands increased roughly fivefold during the 20th century, and the current global irrigated landscape continues to evolve⁴⁶. The three largest crop irrigators globally are China (53.8 Mha), India (57.3 Mha), and the USA (27.9 Mha)⁴⁷, with rice and maize as the primary irrigated crops. However, these countries are among the regions that are projected to suffer increasing freshwater limitations under the majority of the present climate change scenarios. Recent analyses have estimated that a reversion of 20–60 Mha of cropland from irrigated to rainfed management or from full to supplementary irrigation is required by the end of the century in these three countries to balance the irrigation water supply and demand. While there is potential to increase the irrigated area of wheat and thus reduce SWS impacts, this increase must be accompanied by reductions in other current crops (e.g., rice, maize, and cotton) and/or increases in the irrigation efficiency. Additionally, the alleviating effect of irrigation on SWS event impacts is likely to be limited, as any SWS event intrinsically includes at least a 12-month drought period before the harvest. It may be assumed that during SWS events, the availability of water resources for irrigation in many regions is more limited than in normal years.

Directly accounting for changes in energy prices, considered the second most important factor affecting the cost of cereal production^{10,48} after climate was not explicitly considered here. Energy prices play a fundamental role in the cost of agricultural inputs, as energy and fertilizer prices are highly correlated⁴⁹. However, both the globally increasing demand for energy and the efforts to curb the use of fossil fuels will likely increase energy prices not decrease them. With ongoing political conflicts and sanctions on major oil- and gas-producing countries, volatility in energy and crop prices is unlikely to decrease in the short term⁵⁰.

The derived relation between SWS events and price hikes in wheat encompasses multiple causal factors that may not be solely related to actual yield reductions. Since yield reporting is more prone to reporting distortions compared to market prices, the yield analysis has been by-passed here in favor of a direct relation between SWS and price indicators such as WPI and FPI less prone to reporting distortions. However, market prices are undoubtedly influenced by speculations and uncertainties in the response of cereal producing countries during SWS events even when yield reductions are minor.

Regardless of the above-listed assumptions, the SWS–wheat price relations could be considered robust and warrant their inclusion in projected impacts of the SWS-affected area on crop prices. In light of the 2022 crop price volatility, the projected increase in space-time coherent SWS occurrence cannot be overlooked in any estimates of future price levels, at least in the case of wheat. The sensitivity of wheat prices to SWS occurrence stems from the fact that out of the three main cereal crops, wheat is grown mostly under the least favorable soil moisture conditions (Fig. 1c) and cannot be readily replaced by drought-resilient crops. The sensitivity of wheat prices to the SWS extent can benefit from a systematic research focus because wheat is the most important crop in terms of area, calorie supply and volume of international trade (Fig. 1a).

Materials and Methods

The concept of SWS events⁹, which combines three time scales of the standardized precipitation evapotranspiration index (SPEI)⁵¹ is used here to specifically target the critical water shortage time frames for crop production (Table S1). An SWS event occurs when a negative soil moisture anomaly satisfies three conditions: (i) simultaneously persists during most of the growing season for the specific cereal, (ii) peaks during the critical yield-forming period, and (iii) occurs against the backdrop of a long-term water anomaly that reduces regional water resources in general (Table S1). The concept of SWS events enabled the determination of spatial and temporal extents of SWS (e.g., Fig. S2) from climate data and the assessment of the functional relation between water scarcity and cereal prices. The total cereal growing areas and global price response were aggregated here through a set of drought-cereal price models. The main advantage of this method is the ability to consider SWS events as they occur across all cereal-growing areas simultaneously.

The area of maize, rice and wheat production is unevenly distributed globally. However, well-defined production regions within the global arable land (Fig. 1a) are present, as shown in Fig. S1. An increase in SWS events in these regions may significantly increase the probability of experiencing SWS in key producing areas simultaneously (or near simultaneously), as has been shown in earlier case studies targeting wheat⁹. The primary advantage of the SWS concept is that it allows the likelihood of multiple rice–maize–wheat-producing areas experiencing synchronized or/and sequenced SWS events to be analyzed. In each region and for each crop, the water scarcity (as defined in Table S1) occurrence over the four months preceding the typical local harvest date of the given crop was quantified. The probability of SWS events between 1861 and 2100 was based on the standardized precipitation evapotranspiration index (SPEI). In climate studies, the SPEI accounts for both precipitation and potential evapotranspiration

(PET) when assessing the onset and magnitude of a drought. A global 0.5° grid was used, and a given location within the grid was defined as an area affected by water scarcity if both the short-term SPEI impacting the target crop production and the long-term SPEI affecting the water resource availability occurred in each grid cell with water scarcity conditions based on the above-predefined magnitudes (Table S1). Occurrences of SWS during the 1901–2021 period were first evaluated using the CRU dataset⁵², which represents “observed” SWS events. Then, the annual SWS-affected area was considered a predictor of crop prices, and SWS–price models were developed and evaluated (Fig. 1b). The SWS probability from 1861 to 2100 was estimated using the outputs of 27 climate models from the fifth phase and 31 models from the sixth phase of the Coupled Model Intercomparison Project—CMIP5 (Table S3) and CMIP6 (Table S4), respectively. Both CMIP5 and CMIP6 data were used to determine how much the final results depend on the climate model ensemble selected. The SWS occurrence was examined under three emission pathways for CMIP6 (SSP1-2.6; 2-4.5 and 5-8.5) and corresponding representative concentration pathways or RCPs (RCP2.6; 4.5 and 8.5) in the case of CMIP5: (i) SSP1-2.6 and RCP2.6 more or less correspond to the implementation of the 2015 Paris Agreement (26); (ii) SSP2-4.5 and RCP4.5 correspond to the “average” pathway; and (iii) SSP5-8.5 and RCP8.5 correspond to a high-emission world. This approach allowed us to estimate the effect of climate change mitigation on future price levels.

Crop production areas

The total arable land was considered and SWS occurrences in grids where the target crop is grown⁵³ (i.e., maize, rice, and wheat grids—Fig. S1) were first determined. Weights were assigned to each grid according to the acreage of arable land, and each grid was then weighted based on its share of the total area of the target crop. The area of the individual crop grids constituted areas where the crops have been produced⁵⁴. This area reached approximately 171 Mha for maize, 158 Mha for rice and 218 Mha for wheat¹. This approach facilitated estimates of how much of the global area for each crop was affected by SWS in each harvest year. Weighting the specific crop area allowed the effect of water scarcity changes on risk in the current primary production areas to be examined based on either the area or production. To analyze changes in the SWS patterns in the top exporting regions, the cumulative SWS probability in grids in the territories of the ten most important exporters of each crop was examined over the 2010–2020 period, and the grids were weighted according to their share of the entire production area and the production quantity of each crop separately.

Price data

Price data for wheat, maize and rice were used based on the International Grain Council¹¹ in the form of the WPI, maize price index (MPI) and rice price index (RPI). For the given year, the mean value of any given index was used. These price indices cover the 2000–2021 period with the index value in January 2000 set to 100. The FPI, also known as the agricultural price index, is a lagging indicator that has broader economic significance beyond this industry and was used for the 1951–2021 period. The FPI is

estimated monthly by the US Department of Agriculture's National Agricultural Statistics Service (NASS). The annual mean FPI, which closely corresponds to the WPI (Fig. 2c), was used in this study. Both the primary International Grains Council (IGC) data and annual means are provided in the Data section.

Climate data

As mentioned, the simulations of 27 global climate models (Table S3) from the CMIP5 ensemble⁵⁵ and 31 models from the CMIP6 ensemble (Table S4) were analyzed. These simulations included model runs with specific historical, natural, and anthropogenic forcings from 1861 to 2005 in the case of CMIP5 and 1861–2014 in the case of CMIP6 and included 21st century changes in anthropogenic aerosols and greenhouse gases⁵⁶. If a model was associated with multiple simulations, only the first run was analyzed.

All the monthly modeled data (i.e., temperature, precipitation, wind speed, solar radiation, relative humidity and sensible and latent heat flux) were first spatially interpolated from the original model grids to a common grid with a 0.5° resolution and then bias-corrected using the delta change method⁵⁷. The temperature and precipitation were bias-corrected based on the observed 1961–1990 monthly climatology developed by the Climate Prediction Center (CPC)⁵⁸, while the other variables were bias-corrected based on the observed 1961–1990 monthly climatology data developed by the CRU of the University of East Anglia⁵⁹. This bias correction method ensured that the modeled variables were associated with the same monthly climatology as the CPC or CRU observations during the 1961–1990 period.

In addition to the model simulations, the 0.5° gridded monthly observed temperature, precipitation, and PET datasets developed by the CRU (i.e., CRU-TS.4.05)⁵² were used. These datasets were based on observations collected from thousands of weather stations globally from 1901 to 2020, providing a baseline for validating the CMIP5 and CMIP6 model simulations.

Standardized precipitation and evapotranspiration index (SPEI)

The SPEI⁵¹ was adopted, which is a multi-scalar drought index that quantifies the drought intensity on various time scales. The SPEI was computed based on 1, 3, 6 and 12 months of accumulated surface water deficits and surpluses (i.e., precipitation minus PET). The calculation then employed statistical probability distributions to quantify the drought intensity, termed the 1-, 3-, 6-, 9- or 12-month SPEI. The 1-month SPEI is closely related to the shallow-layer soil moisture and can be used to evaluate the short-term drought variability. The 12-month SPEI is closely related to the deep-layer soil moisture and long-term drought variability.

The PET was estimated using the FAO-56 Penman–Monteith method for reference grass⁶⁰ using air temperature, relative humidity, wind speed and solar radiation as inputs. In addition to consistent warming⁶¹, climate models are consistent in showing regional changes in the relative air humidity⁶² and

vapor pressure deficit. The roles of the wind speed and solar radiation in PET are secondary⁶³ in the future. Due to the notable impacts of the temperature and relative humidity, climate models routinely project increasing PET levels⁶⁴.

Values of the 1-, 3-, 6-, 9- and 12-month SPEI were calculated based on the monthly precipitation and PET. The snow-melting module developed by Van der Schrier *et al.*⁶⁵ was also assessed to quantify the impact of snow on the water supply. However, the differences between SWS with and without considering snow melt were non-significant within the growing areas of the three analyzed crops. Therefore, a simplified scheme was implemented that did not account for snow melting. For a given climate model output, the statistical probability distribution parameters⁵¹ used to calculate the SPEI were determined based on the modeled monthly data from 1901–2000. These parameters were subsequently used to calculate SPEI values in each grid cell from 1860–2005 for CMIP5 and 1860–2014 for CMIP6 and under the different future scenarios. The same procedures were applied to calculate the SPEI from 1901–2021 based on the CRU dataset.

Defining severe water scarcity events and drought-sensitive periods

SWS events (Table S1) were first defined to quantify the short- and long-term impacts of water shortages on crops. A grid cell was considered affected by water scarcity only if both the short-term water scarcity indicators (i.e., 1- and 3-month SPEI) and the long-term water scarcity indicators (i.e., 12-month SPEI) reached predefined thresholds (Table S1). These thresholds were adopted based on prior studies⁶⁶, wherein the probability of drought impact occurrence was estimated based on the impacts of drought in individual sectors. Since all three considered crops are grown during part of the year, the crop-specific water scarcity sensitivity periods (SPs) were used. These were defined as the four months prior to the usual crop harvest date (i.e., the period that includes both the peak vegetative stage (i.e., wheat heading and maize and rice flowering) as well as grain filling for each crop. Both stages are sensitive to soil moisture deficits. These four months constitute the time of the most intense growth, including the formation of all yield components. For rice, only the first harvest date during a given season was considered.

When the usual harvest date occurred on or later than the 20th day of the month, the drought index for the harvest month and the three preceding months was used. When the crop was harvested before the 20th day of the harvest month, the drought index for the four months prior to the harvest month was used. This offset was used because the crop harvest date, in practice, follows the physiological maturity by several days or even weeks (in the case of wheat and maize), and the sensitivity of all three crops to drought rapidly decreases at the end of the grain filling stage and after maturity. In fact, drier conditions during harvest are generally beneficial for crop quality and could increase the harvest efficiency. In all calculations, calendar months were used.

Final weighting procedure

For each crop-growing grid cell and year, it was first determined whether the cell and year were affected by SWS ($D_i = 1$) or not ($D_i = 0$) during each crop-growing season based on the thresholds defined in Table S1. For a 1-year window of water scarcity, only events during the harvest year were considered. For a two-year SWS window, a grid was considered affected by water scarcity ($D_i = 1$) if the SWS thresholds were met either during the harvest year or during the previous harvest year. Similarly, a three-year window of water scarcity categorized a grid as experiencing SWS if the conditions were met during the SPs of the harvest year or during any of two preceding years. The use of 1-, 2- and 3-year windows allowed us to examine the impacts of a sequence of severe (extreme) water scarcity events, as was, for example, the case of wheat production and, to a certain extent, maize production caused by the 2010 droughts in Russia and India and the 2012 drought in the USA. The area affected by severe or extreme drought was then determined as follows:

$$\text{Area affected by drought is given as } 100 \times \frac{\sum_{i=1}^n Diwi}{\sum_{i=1}^n wi}, (1)$$

where w_i is the share of the global wheat area (for wheat calculations). Variations in the grid size due to the latitude were also accounted for.

Relating SWS to crop price models

The relation between SWS occurrence and price is complex. In the development of the SWS–crop price model, values of the crop-specific price indices (i.e., WPI, MPI, and RPI) were used. A wide range of SWS predictors was systematically explored and assessed in hierarchical order. This included the SWS extent in arable land, the given cereal-growing area, and the given cereal-growing area within its 10 main exporters. The effects of SWS events on prices can vary over time and can materialize with a significant time lag. To capture this complexity, different time lags were considered, including analysis of i) the SWS extent window and ii) cereal price time lag. In any model, the SWS effect on price accumulated over three windows was considered, i.e., the given season ($n = 1$ or $w1$), the given season and its preceding season ($n; n-1 = w2$) and the given season and the two previous seasons ($n + 1; n; n-1 = w3$). The cereal price lag accounted for the offset between SWS and price formation. In total, four time lags were considered with lag0 indicating the annual price responding to SWS in the given year, while lag1 expects the cereal price to lag the SWS extent by 1 year. At the same time, both the cereal price index and SWS values and the first-order residuals were used. For each crop, $3 \times 3 \times 4 \times 2 = 72$ linear models were formulated and evaluated, and the best performing models are shown in Fig. 1b, Fig. S3 and Table S2.

Combinations of SWS occurrence (non-trended and detrended), price lags of 0–3 years and different sizes of SWS windows from 1–3 years were set. Roughly, the 3-year lag sets the upper bound to offset any storage capacity for grains. Under each such combination, the Pearson correlation coefficient (R), Spearman rank coefficient, Theil coefficient and RMSE were calculated. The model performance was captured for all three crops as shown in Fig. 1b. The Taylor diagrams provided justification for only using wheat in the analysis, as the rice models performed rather poorly, and the maize models explained less than half of the price variability from SWS variability as expected.

In the case of wheat, the 15 best performing models were iteratively combined into the best performing ensemble based on the highest R^2 and lowest RMSE values (Fig. S3,4). The iterative process resulted in a final ensemble of five models (Fig. 2a and Table S2). These five models based only on SWS were individually evaluated using the Pearson correlation coefficient by bootstrapping with 10000 repeats (Fig. 2b).

A subset of 5 models was optimized by weights to improve R^2 . These weights were calculated by the minimum least square method with positive results, namely, the weights conformed with the defined combination of the models given in Table S3. The final model (M) applied these weights. The weighted values are marked as black points in Fig. 2a and as time series in Fig. 3. Confidence intervals of the linear regression and WPI values are also presented.

The finale 5-model subset was used to estimate the price levels between 1951 and 2021 using the CRU dataset, resulting in control period benchmark values of the price index, and they were compared to the FPI. Fig. S4 shows estimates of the FPI from 2000–2021 obtained with the model ensemble trained only on the 1951–2000 period.

The grain prices were estimated over the control periods of both CMIP6 (31 runs in Fig. 2) and CMIP5 (27 runs in Fig. S5) as annual and 10-year means. The CMIP6- and CMIP5-based price estimates are presented as the mean and confidence intervals. The estimates of the price model based on the CRU data were higher on average than the climate model-based estimates, as shown by the filtered data given by the 10-year running means in Fig. 3a. The uncertainty band is a composite of the 10%/90% uncertainty in the linear regression and the 0.05/0.95 quantile of the 31 (27) model outputs based on the CMIP6 (CMIP5) GCMs.

Figure 3c shows the relation between the expected change in the global temperature and the estimated wheat prices based on the 31 global climate model outputs. Figure 3c on the left shows estimates of all changes in the mean annual temperature under all scenarios of all individual global models from the entire ensemble for all years from 1951 to 2100 and the price estimates computed based on these values by the final model M. The curves denote the 0.1, 0.5 (median) and 0.9 quantiles of the price estimates for a given temperature change. The right-hand side panel of the graph shows the averages of the price estimates from the entire ensemble of the global models for each individual year between 1951 and 2100.

Declarations

Acknowledgments

The authors thank Anastassios Haniotis for the valuable comments and suggestions. The study has been supported by AdAgriF - Advanced methods of greenhouse gases emission reduction and sequestration in agriculture and forest landscape for climate change mitigation“

(CZ.02.01.01/00/22_008/0004635). Rothamsted Research received grant-aided support from the Biotechnology and Biological Sciences Research Council (BBSRC) through the Delivering Sustainable Wheat strategic program (BB/X011003/1).

Data availability

The datasets generated during and/or analyzed in this study are available from the corresponding author and after review will be put in the public data repository.

Code availability

The source code is available from the corresponding author upon reasonable request.

References

1. FAO. FAOSTAT. <https://www.fao.org/faostat/en> (2022).
2. Mekonnen, M. M. & Hoekstra, A. Y. The green, blue and grey water footprint of crops and derived crop products. *Hydrol. Earth Syst. Sci.* 15, 1577–1600 (2011).
3. FAO. *The future of food and agriculture - Trends and challenges*. (2017).
4. OECD, Food & of the United Nations, A. O. *OECD-FAO Agricultural Outlook 2020–2029*. (2020). doi:<https://doi.org/10.1787/1112c23b-en>.
5. Janssens, C. *et al.* Global hunger and climate change adaptation through international trade. *Nat. Clim. Chang.* 2020 109 10, 829–835 (2020).
6. Zhu, P. *et al.* Warming reduces global agricultural production by decreasing cropping frequency and yields. *Nat. Clim. Chang.* 2022 1211 12, 1016–1023 (2022).
7. Baker, J. S. *et al.* Evaluating the effects of climate change on US agricultural systems: sensitivity to regional impact and trade expansion scenarios. *Environ. Res. Lett.* 13, 064019 (2018).
8. Heinicke, S., Frieler, K., Jägermeyr, J. & Mengel, M. Global gridded crop models underestimate yield responses to droughts and heatwaves. *Environ. Res. Lett.* 17, 044026 (2022).
9. Trnka, M. *et al.* Mitigation efforts will not fully alleviate the increase in water scarcity occurrence probability in wheat-producing areas. *Sci. Adv.* 5, (2019).
10. Conceição, P. & Mendoza, R. U. Anatomy of the global food crisis. *Third World Q.* 30, 1159–1182 (2009).
11. IGC. IGC Grains and Oilseeds Index. <https://www.igc.int/en/markets/marketinfo-goi.aspx> (2022).
12. World Bank Group. *Special Focus: Food Price Shocks: Channels and Implications. Commodity Markets Outlook, April*. www.worldbank.org/commodities (2019).

13. FAO, WFP & IFAD. *The State of Food Insecurity in the World 2012: Economic growth is necessary but not sufficient to accelerate reduction of hunger and malnutrition*. (2012).
14. Hasegawa, T. *et al.* A global dataset for the projected impacts of climate change on four major crops. *Sci. Data* 2022 919, 1–11 (2022).
15. Nendel, C. *et al.* Future area expansion outweighs increasing drought risk for soybean in Europe. *Glob. Chang. Biol.* 29, 1340–1358 (2023).
16. Nelson, G. C. *et al.* Climate change effects on agriculture: Economic responses to biophysical shocks. *Proc. Natl. Acad. Sci. U. S. A.* 111, 3274–3279 (2014).
17. Hasegawa, T. *et al.* Risk of increased food insecurity under stringent global climate change mitigation policy. *Nat. Clim. Chang.* 2018 888, 699–703 (2018).
18. Portmann, F. T., Siebert, S. & Döll, P. MIRCA2000-Global monthly irrigated and rainfed crop areas around the year 2000: A new high-resolution data set for agricultural and hydrological modeling. *Global Biogeochem. Cycles* 24, (2010).
19. Myers, S., Fanzo, J., Wiebe, K., Huybers, P. & Smith, M. Current guidance underestimates risk of global environmental change to food security. *BMJ* 378, (2022).
20. Van Meijl, H. *et al.* Comparing impacts of climate change and mitigation on global agriculture by 2050. *Environ. Res. Lett.* 13, 064021 (2018).
21. Frieler, K. *et al.* Understanding the weather signal in national crop-yield variability. *Earth's Futur.* 5, 605–616 (2017).
22. Green, R. *et al.* The effect of rising food prices on food consumption: systematic review with meta-regression. *BMJ* 346, (2013).
23. Smith, L. C. & Subandoro, A. *Measuring Food Security Using Household Expenditure Surveys. Food security in Practice technical guide series*. vol. 3 (International Food Policy Research Institute, 2007).
24. Lele, U. *et al.* Measuring food and nutrition security: An independent technical assessment and user's guide for existing indicators. Rome Food Secur. Inf. Network, Meas. Food Nutr. Secur. Tech. Work. Gr. 177, (2016).
25. UN-Habitat, U. N. *United Nations UN-Habitat World Cities Report - Envisaging the Future of Cities. United Nations Human Settlements Programme (UN-Habitat)* (2022).
26. Dadi, W., Mulegeta, M. & Simie, N. Urbanization and its effects on income diversification of farming households in Adama district, Ethiopia. *Cogent Econ. Financ.* 10, (2022).
27. de Janvry, A. & Sadoulet, E. Subsistence farming as a safety net for food-price shocks. *Dev. Pract.* 21, 472–480 (2011).
28. Fodor, N. *et al.* Integrating Plant Science and Crop Modeling: Assessment of the Impact of Climate Change on Soybean and Maize Production. *Plant Cell Physiol.* 58, 1833–1847 (2017).
29. Mourtzinis, S., Specht, J. E. & Conley, S. P. Defining Optimal Soybean Sowing Dates across the US. *Sci. Reports* 2019 919, 1–7 (2019).

30. Marchand, P. *et al.* Reserves and trade jointly determine exposure to food supply shocks. *Environ. Res. Lett.* 11, 095009 (2016).
31. Hertel, T., Elouafi, I., Tanticharoen, M. & Ewert, F. Diversification for Enhanced Food Systems Resilience. in *Science and Innovations for Food Systems Transformation* (eds. von Braum, J., Afsana, K., Fresco, L. O. & Hassan, M. H. A.) 207–216 (Springer, 2023). doi:10.1007/978-3-031-15703-5.
32. Janssens, C. *et al.* Global hunger and climate change adaptation through international trade. *Nat. Clim. Chang.* 2020 109 10, 829–835 (2020).
33. Schewe, J., Otto, C. & Frieler, K. The role of storage dynamics in annual wheat prices. *Environ. Res. Lett.* 12, 054005 (2017).
34. Godfray, H. C. J., Mason-D’croz, D. & Robinson, S. Food system consequences of a fungal disease epidemic in a major crop. *Philos. Trans. R. Soc. B Biol. Sci.* 371, (2016).
35. Peng, W. *et al.* A review of historical and recent locust outbreaks: Links to global warming, food security and mitigation strategies. *Environ. Res.* 191, 110046 (2020).
36. Tadasse, G., Algieri, B., Kalkuhl, M. & von Braun, J. Drivers and triggers of international food price spikes and volatility. in *Food Price Volatility and Its Implications for Food Security and Policy* (eds. Kalkuhl Matthias, von Braun Joachim & Torero Maximo) 59–82 (Springer International Publishing, 2016). doi:10.1007/978-3-319-28201-5_3.
37. Headey, D. Rethinking the global food crisis: The role of trade shocks. *Food Policy* 36, 136–146 (2011).
38. Glauber, J. W. & Laborde Debucquet, D. How will Russia’s invasion of Ukraine affect global food security? in *The Russia-Ukraine conflict and global food security* (eds. Glauber, J. W. & Laborde Debucquet, D.) 196 (International Food Policy Research Institute, 2023). doi:10.2499/9780896294394.
39. Chepelliev, M., Maliszewska, M. & Pereira, M. S. E. Effects on trade and income of developing countries. in *The Impact of the War in Ukraine on Global Trade and Investment* (ed. Ruta, M.) 11–26 (World Bank Group, 2022).
40. Lobell, D. B. Climate change adaptation in crop production: Beware of illusions. *Glob. Food Sec.* 3, 72–76 (2014).
41. Challinor, A. J. *et al.* A meta-analysis of crop yield under climate change and adaptation. *Nat. Clim. Chang.* 2014 44 4, 287–291 (2014).
42. Manderscheid, R. & Weigel, H. J. Drought stress effects on wheat are mitigated by atmospheric CO₂ enrichment. *Agron. Sustain. Dev.* 2007 272 27, 79–87 (2007).
43. Jin, Z., Ainsworth, E. A., Leakey, A. D. B. & Lobell, D. B. Increasing drought and diminishing benefits of elevated carbon dioxide for soybean yields across the US Midwest. *Glob. Chang. Biol.* 24, e522–e533 (2018).
44. Schauburger, B. *et al.* Consistent negative response of US crops to high temperatures in observations and crop models. *Nat. Commun.* 2017 81 8, 1–9 (2017).

45. Dai, A., Zhao, T. & Chen, J. Climate Change and Drought: a Precipitation and Evaporation Perspective. *Curr. Clim. Chang. Reports* 2018 43 4, 301–312 (2018).
46. Siebert, S. *et al.* A global data set of the extent of irrigated land from 1900 to 2005. *Hydrol. Earth Syst. Sci.* 19, 1521–1545 (2015).
47. Thenkabail, P. S. *et al.* Global irrigated area map (GIAM), derived from remote sensing, for the end of the last millennium. *Int. J. Remote Sens.* 30, 3679–3733 (2009).
48. Enghiad, A., Ufer, D., Countryman, A. M. & Thilmany, D. D. An Overview of Global Wheat Market Fundamentals in an Era of Climate Concerns. *Int. J. Agron.* 2017, (2017).
49. Kalkuhl, M., von Braun, J. & Torero, M. Food price volatility and its implications for food security and policy. *Food Price Volatility Its Implic. Food Secur. Policy* 1–626 (2016) doi:10.1007/978-3-319-28201-5/COVER.
50. Wang, Y., Bouri, E., Fareed, Z. & Dai, Y. Geopolitical risk and the systemic risk in the commodity markets under the war in Ukraine. *Financ. Res. Lett.* 49, 103066 (2022).
51. Vicente-Serrano, S. M., Beguería, S. & López-Moreno, J. I. A Multiscalar Drought Index Sensitive to Global Warming: The Standardized Precipitation Evapotranspiration Index. *J. Clim.* 23, 1696–1718 (2010).
52. Harris, I., Jones, P. D., Osborn, T. J. & Lister, D. H. Updated high-resolution grids of monthly climatic observations – the CRU TS3.10 Dataset. *Int. J. Climatol.* 34, 623–642 (2014).
53. Ramankutty, N., Evan, A. T., Monfreda, C. & Foley, J. A. Farming the planet: 1. Geographic distribution of global agricultural lands in the year 2000. *Global Biogeochem. Cycles* 22, 1003 (2008).
54. Hoekstra, A. Y., Mekonnen, M. M., Chapagain, A. K., Mathews, R. E. & Richter, B. D. Global Monthly Water Scarcity: Blue Water Footprints versus Blue Water Availability. *PLoS One* 7, e32688 (2012).
55. Taylor, K. E., Stouffer, R. J. & Meehl, G. A. An Overview of CMIP5 and the Experiment Design. *Bull. Am. Meteorol. Soc.* 93, 485–498 (2012).
56. van Vuuren, D. P. *et al.* The representative concentration pathways: An overview. *Clim. Change* 109, 5–31 (2011).
57. Feng, S. *et al.* Projected climate regime shift under future global warming from multi-model, multi-scenario CMIP5 simulations. *Glob. Planet. Change* 112, 41–52 (2014).
58. Fan, Y. & van den Dool, H. A global monthly land surface air temperature analysis for 1948–present. *J. Geophys. Res. Atmos.* 113, 1103 (2008).
59. New, M., Hulme, M. & Jones, P. Representing Twentieth-Century Space–Time Climate Variability. Part I: Development of a 1961–90 Mean Monthly Terrestrial Climatology. *J. Clim.* 12, 829–856 (1999).
60. Allen, R. G., Pereira, L. S., Raes, D., Smith, M. & W, a B. *Crop evapotranspiration - Guidelines for computing crop water requirements*. FAO Irrigation and drainage paper 56 (1998) doi:10.1016/j.eja.2010.12.001.
61. Collins, M. *et al.* Long-term climate change: Projections, commitments and irreversibility. in *Climate Change 2013: The Physical Science Basis. Contribution of Working Group I to the Fifth Assessment*

Report of the Intergovernmental Panel on Climate Change (eds. Stocker, T. F. et al.) 1029–1136 (Cambridge University Press, 2013).

62. Sherwood, S. & Fu, Q. A drier future? *Science* (80-). 343, 737–739 (2014).
63. Fu, Q. & Feng, S. Responses of terrestrial aridity to global warming. *J. Geophys. Res. Atmos.* 119, 7863–7875 (2014).
64. Scheff, J. & Frierson, D. M. W. Scaling Potential Evapotranspiration with Greenhouse Warming. *J. Clim.* 27, 1539–1558 (2014).
65. van der Schrier, G., Efthymiadis, D., Briffa, K. R. & Jones, P. D. European Alpine moisture variability for 1800–2003. *Int. J. Climatol.* 27, 415–427 (2007).
66. Blauhut, V., Gudmundsson, L. & Stahl, K. Towards pan-European drought risk maps: Quantifying the link between drought indices and reported drought impacts. *Environ. Res. Lett.* 10, 014008 (2015).

Footnotes

1. * The increase was calculated using the wheat, maize, and rice price index values in March 2007 and 2010 relative to March 2008 and 2011, respectively.

Figures

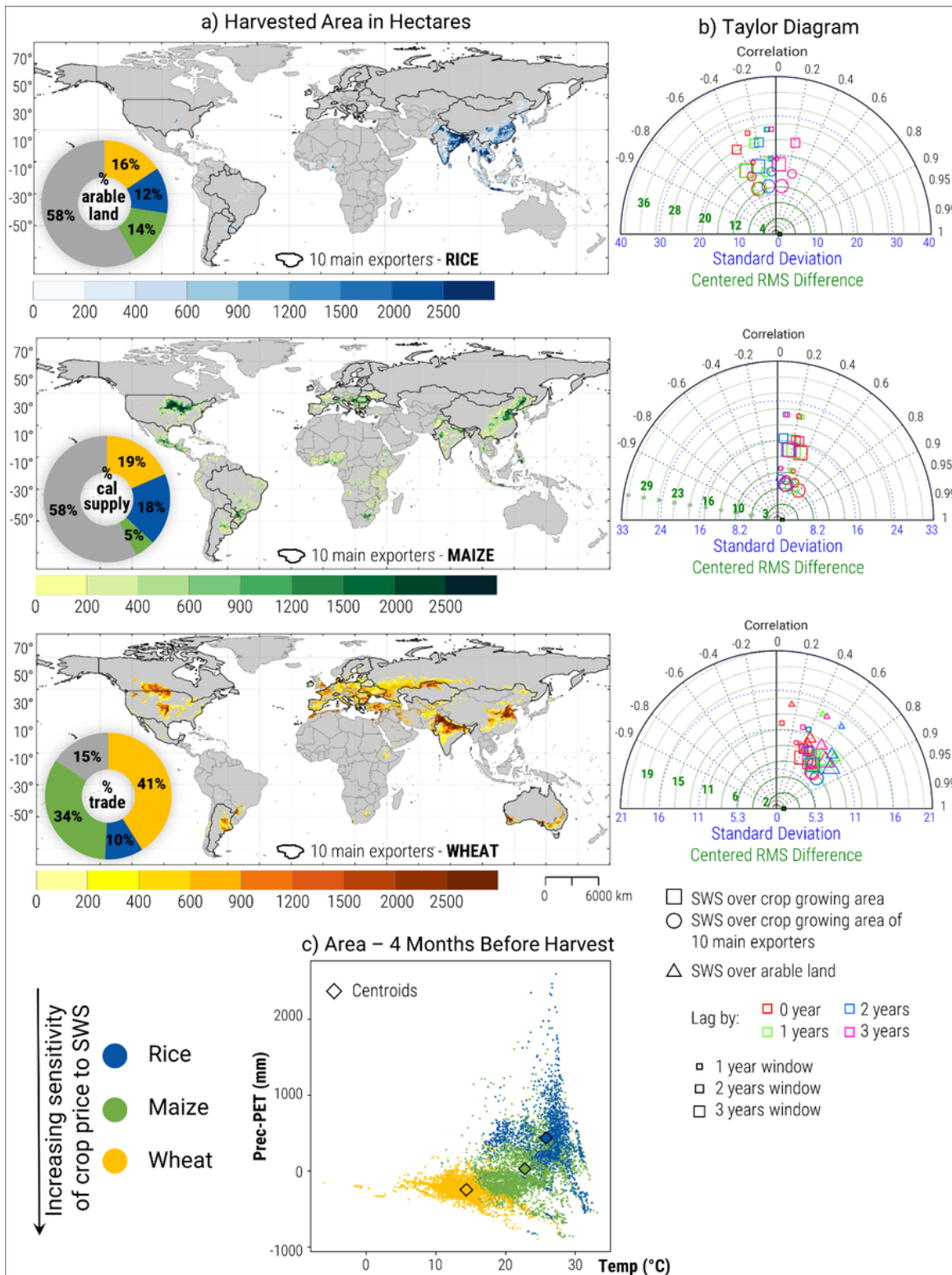


Figure 1

a) Main areas of rice/maize/wheat production with the borders of the 10 top exporting countries highlighted. The doughnut charts indicate the share of the three major crops in the global arable land area, calorie supply and agriculture commodity trade. b) Results of the fit of severe water scarcity (SWS) and price index to form crop price models in the form of Taylor diagrams, where different areas, lags (0–3 years) and time windows (1–3 years) of SWS are considered. The diagram visualizes the Pearson

correlation coefficient (black), standard deviation (blue) and centered root mean square difference (green). The black dot indicates the perfect fit model with a Pearson correlation $R=1$ and root-mean squared error or RMSE=0. c) Basic climatological characteristics of the climate model grids growing rice, maize and wheat showing their mean temperatures (X-axis or abscissa) and the sum of the differences in precipitation and PET during the 4 months before the harvest (Y-axis or ordinate).

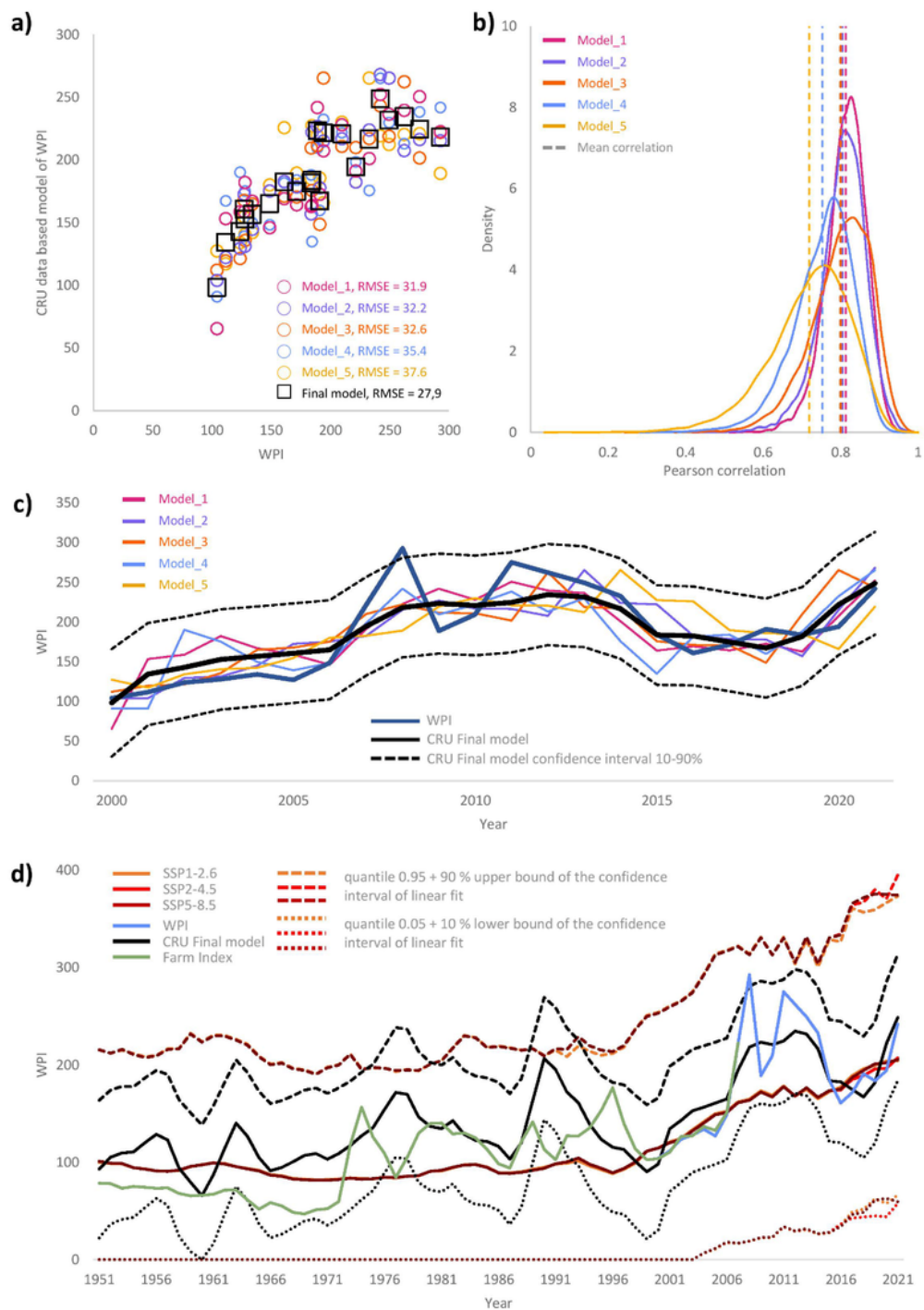


Figure 2

a) Comparison of the reported wheat price index (WPI) values on the X-axis and its estimates using the ensemble of the 5 best performing linear models driven by the CRU derived SWS estimates on the Y-axis; b) bootstrapping tests of the 5 models (Table S4); c) time series of the reported and estimated WPI values using the 5 best performing models and their final ensemble for the 2000–2021 period; d) reported WPI and farm price index (FPI) annual mean values for the 1951–2021 period compared to the CRU data and CMIP6-based price estimates including confidence intervals.

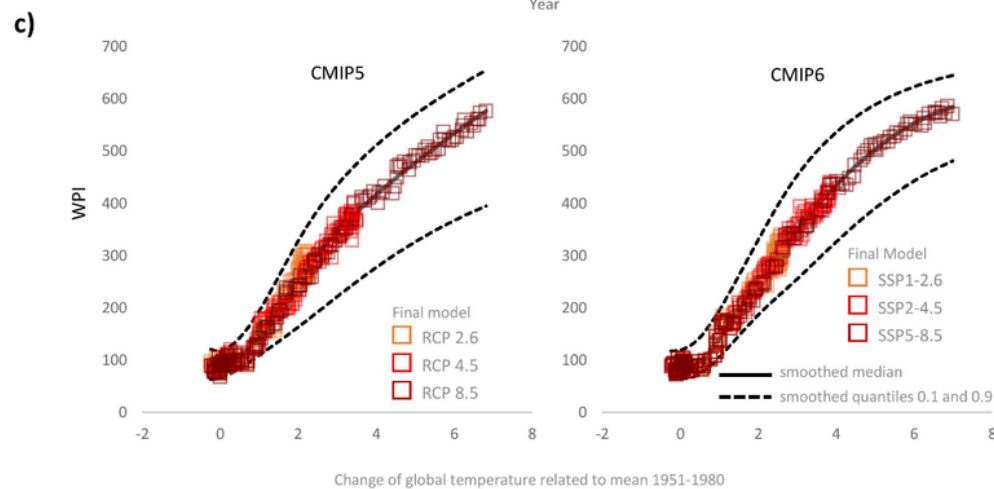
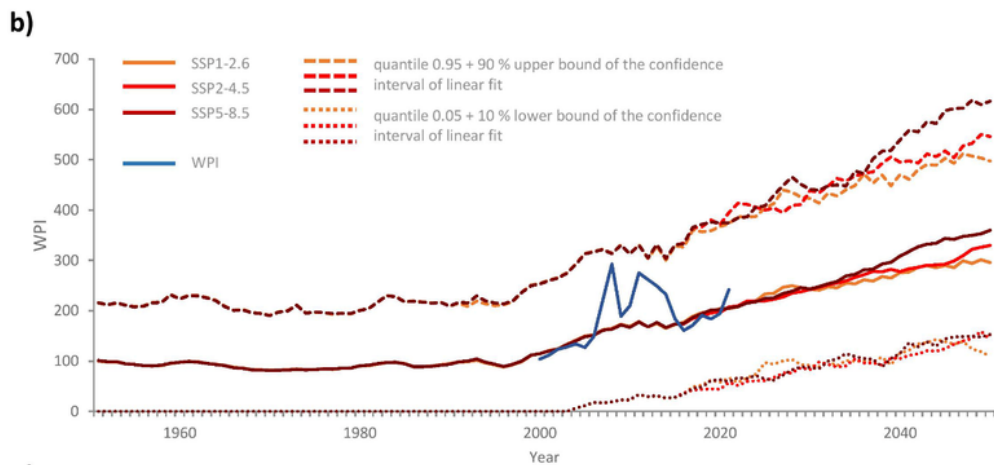
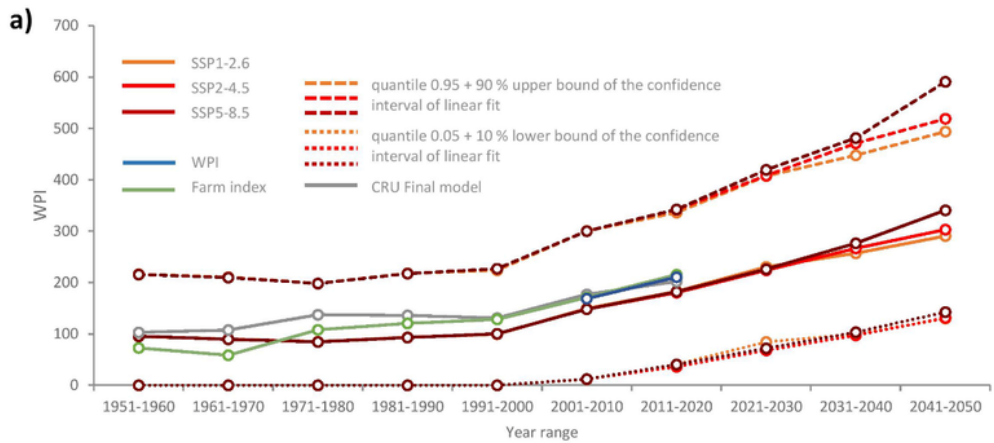


Figure 3

a) Ten-year mean values of the reported wheat price index (WPI) for 2000–2021 and farm price index (FPI) for 1951–2021 with the estimated values based on the CRU data for 1951–2021 as well as the results of the CMIP6 model ensemble for 1951–2050; b) the same as (a) but showing annual values; c) summary of the expected WPI related to the change in the global mean temperature estimated using the CMIP5 and CMIP6 models.

Supplementary Files

This is a list of supplementary files associated with this preprint. Click to download.

- [Supplement.docx](#)